Gut Microbiome-Mediated Changes in Bone Metabolism Upon Infrared Light Exposure in Rats

Yueying Lu
Beihang University
Jianlou Yang
Beihang University
Yuming Fu (fuyuming@buaa.edu.cn)
Beihang University https://orcid.org/0000-0003-0289-2703
Hong Liu
Beihang University

Research

Keywords: Gut microbiome, Bone health, Infrared radiation, Healthy light source

Posted Date: June 2nd, 2020

DOI: https://doi.org/10.21203/rs.3.rs-31291/v1

Version of Record: A version of this preprint was published at Journal of Photochemistry and Photobiology B: Biology on April 1st, 2021. See the published version at https://doi.org/10.1016/j.jphotobiol.2021.112156.

Abstract

Background Adequate sunlight exposure helps reduce bone loss and is important to bone health. Currently, about 90% of the world population spends a major portion of daily life under artificial lighting. Unlike sunlight, LED white light, the main source of artificial lighting, has no infrared radiation, which is known to be beneficial to human health. In artificial lighting environments, infrared supplementation may be used to simulate the effects of sunlight on bone metabolism.

Results Here, we supplemented white LED exposure with infrared light in normal and ovariectomized rats for three consecutive months and examined bone turnover, bone mass, and bone density. We also analyzed the structure and function of gut microbiota in the rats. Infrared supplementation significantly reduced the abundance of Saccharibacteria and increased the abundance of *Clostridiaceae 1* and *Erysipelotrichaceae* bacteria. Our results indicate that changes in the gut microbiome correlate well with bone mass and bone metabolism.

Conclusions Our work demonstrates that infrared supplementation can have a positive effect on rat bone metabolism by affecting gut microbiota. Our findings will be important considerations in the future design of healthy lighting environments that prevent or possibly ameliorate osteoporosis.

Introduction

In present times, the majority of individuals spend more than 90% of their time indoors under artificial lighting. Working and living in an artificially illuminated environment for long durations are known to have a negative impact on bone health, leading to bone loss, osteomalacia, and osteoporosis [1]. For example, young submarine crews completing long-haul missions exhibit significant decreases in bone strength [2]. Several studies have shown that these negative effects on bone metabolism are a result of the lack of beneficial spectra in artificial light sources compared to full spectrum sunlight [3]. Ultraviolet irradiation (UVR) and infrared radiation (IR) are considered the major healthy light regions in the sunlight spectrum [4]; however, white light-emitting diodes (LED), one of the current main indoor lighting sources, does not include these two types of light for energy saving reasons. Developing healthy and cost-effective artificial lighting strategies is needed to maintain human bone health for the vast number of individuals who spend significant durations indoors.

Most recent studies on improving artificial lighting have focused on the positive effects of supplemental UVR on bone metabolism. Several of these reports have demonstrated that UVR plays a critical role in maintaining bone health through increasing the endogenous generation of vitamin D [2,5.6]. Interestingly, a recent study showed that UVB light can rapidly modulate the gut microbiome in response to increases in vitamin D [7]. Photobiomodulation has a therapeutic effect on inflammation and neurological disorders [8]. Exposure to UVB radiation is likely to first change the skin microbiome, leading to local changes in innate and adaptive immune cells. These cells are then transported to more systematic sites, including the gut, where the media they release in turn form the composition of the gut microbiome [7,9,10]. This indicates that light may be used to affect intestinal homeostasis and subsequently influence bone metabolism.

Pinheriro *et al.*[11] found that IR therapy has a positive effect on bone defect healing, regeneration and repair. Ueda *et al.* [12] showed that a low frequency pulsed IR source can significantly stimulate bone nodule formation in rat calvarial cells. In addition, the combination of IR and treadmill training can work synergistically to enhance muscle performance and mitigate decreases in femoral bone density, preventing osteoporosis and its related health consequences [13]. Thus, the studies mentioned above suggest that IR can also play an important role in bone health. However, there is no information available in the literature on IR supplementation to white light LED to simulate the effect of sunlight irradiation on bone. Moreover, it is unclear whether IR supplementation may modulate the gut microbiota-associated bone metabolism.

Here we investigated the effects of long-term IR supplementation to white LED light on the bones using normal and ovariectomized rats. Using 16s amplicon analysis, we found that IR light altered gut microbiota composition and consequently improved bone metabolism. Based on our results, we propose mechanism of skin-gut-bone axis-regulated bone metabolism under IR supplementation. Our findings not only provide a promising strategy for developing artificial lighting that improves bone health, but also reveal that IR supplementation can exert its benefits on bone health by regulating the gut microenvironment of humans.

Methods

Animals and experimental design

Forty 8-week-old female Sprague-Dawley (SD) rats (Beijing Weitong Lihua Animal Experiment Technology Co., Ltd.) weighing 200 ± 20 g were used in this study. Half of the rats were ovariectomized to establish a rat model of bone loss. During the experiment, each group of rats was housed in a plastic squirrel cages (n = 10 per group). The cage covers were light-permeable, breathable iron mesh. Ordinary feed and drinking water were available ad libitum. The animals were maintained under controlled conditions (12-h light-dark cycle, 24 ± 2°C, 30–55% relative humidity). The weights of the rats were monitored once a week.

The rats were randomly divided into four groups: Normal, ovariectomized (Ovx), Normal+IR, and Ovx+IR. The experiment was started after the rats in each group were adaptively fed for two weeks, at which time all four groups were provided illumination from 10:00 to 22:00. The Normal and Ovx rats conducted all physiological activities under LED white light, while the Normal+IR and Ovx+IR rats were illuminated with LED white light, supplemented with a low-dose IR light exposure. The IR supplementary light irradiation was carried out from 14:00 to 14:30 every day. The experiment lasted for three months. The light intensity and IR light intensity of the active area of the rats were detected by optical fiber spectrometry every week. The illuminance of the active area in the feeding box was 1000 lux. The peak of the IR supplementary light was 830 nm and the intensity was about 100 mW/cm^2 (Fig. 1b). During the experiment, serum was taken once in a month, and the total body bone mass content (BMC) and bone mineral density (BMD) of each rat were measured.

Serum metabolite determination

At each stage of the experiment, blood samples were drawn from the tail vein of each rat after 12 hours of fasting and immediately collected in a centrifuge tube. The samples were then centrifuged at 4200× g for 15 minutes using a cryogenic centrifuge. The plasma supernatant was collected and stored at −20℃ until analysis to avoid repeated freeze-thaw cycles. The concentration of bone metabolism markers, including 1,25-dihydroxyvitamin D3 (1,25-(OH)2-D3), bone-specific alkaline phosphatase (BALP), and tartrate-resistant acid phosphatase (TRACP), were detected using an ELISA kit (Beijing Ruigebo Technology Development Co., Ltd.) according to the manufacturer's protocol.

Dual energy X-ray (DXA)

The rats were deeply anesthetized with pentobarbital sodium solution at a mass fraction of 1% by intraperitoneal injection. The rats were then scanned with a dual-energy X-ray bone densitometer (Hologic Discovery A). The BMC and BMD of each rat were measured using the method described by Zhuang *et al.*[14]. Before measurements, a tissue calibration scan was performed with a Hologic phantom. All measurements were performed by the same operator, followed by software analysis of the DXA data.

DNA extraction, bacterial enumeration, and Illumina sequencing

Fresh stool was collected from the colon of rats at sacrifice and immediately frozen and stored at −80°C. Bacterial genomic DNA was extracted from the frozen stool samples with a DNA extraction kit, according to the manufacturer's instructions. The V3-V4 region of the 16S rRNA (341F-805R, F: GATCCTACGGGAGGCAGCA; R: GCTTACCGCGGCTGCTGGC) was amplified by thermal cycling consisting of initial denaturation at 98℃ for 1 min, followed by 30 cycles of denaturation at 98℃ for 10 s, annealing at 50°C for 30 s, and elongation at 72°C for 60 s, and, finally, holding at 72°C for 5 min. High-throughput pyrosequencing of the PCR products was performed on an Illumina MiSeq/HiSeq2500 platform (Biomarker Technologies Co., Ltd., Beijing, China), and 250 bp paired end reads were generated. Approximately 2.02 GB of raw reads were generated by Illumina sequencing.

Bacterial community analysis and functional prediction

Vsearch 2.8.1 software [15] was used to merge the two ends of the original data obtained by high-throughput sequencing, and remove the primers and redundancy. Non-cluster denoising was performed on the data using Usearch10 software. A high-quality filtered sequence with more than 97% consistency was clustered to obtain operational taxonomic units (OTUs), standardized with the minimum sample data amount. The OTUs were then annotated based on the SILVA taxonomy database[16].

The corr.test function (from the psych package) in the R language was used to separately calculate the Spearman correlation coefficients of the OTUs with relative abundance > 100 in a single group and to obtain the correlation coefficient matrix and P-value matrix. Next, based on the Spearman correlation matrix

and the corrected P-value matrix, an intestinal flora interaction network was established. We used thresholds of 0.7 and 0.05 for the Spearman correlation coefficient and P-value, respectively. To describe the topology of the resulting network, a set of metrics (average, network diameter, graph density, modularity, average clustering coefficient, and average path length) were calculated [17]. Using the interactive platform Gephi [18] and Fruchterman Reingold layout, the network structure was explored and visualized using an undirected network.

An open-source R package, Tax4Fun, was first used to analyze the enrichment of functional genes of the microbiome of each group [19]. The output from QIIME2 software with the SILVA database extension was used for this analysis. Tax4Fun can survey the functional genes of bacterial communities based on the 16S rRNA sequencing data and provide an accurate approximation of the gene profiles obtained from metagenomic shotgun sequencing methods [20].

Statistical analysis

All statistical analysis of the data was processed and statistically analyzed using R (https://www.r-project.org) [21]. Based on the number of OTUs observed, the chao1 and Shannon_e index were used to assess the richness and diversity of bacteria. Two-way ANOVA was used to assess group differences in alpha diversity measurements of major effects (bone loss and light) and interaction terms. Analysis of similarity (ANOSIM), to assess differences in community composition [22], and principal coordinate analysis (PCoA), to assess ordination, were performed using unweighted Unifrac dissimilarity matrices. The correlation between bone metabolism indexes and bacteria was assessed by Spearman's correlation coefficient.

Differences in the relative abundance of bacteria, serum metabolites, bone mass, and bone density between treatment groups were compared using one-way ANOVA and the Wilkerson rank sum test for multiple comparisons. $P < 0.05$ was considered statistically significant. Significant differences are noted as $*p < 0.05$, $**p < 0.01$, and $***p < 0.001$.

Results

Changes in BMC, BMD, and serum bone metabolism markers after IR supplementation

To examine changes in rat bone health, we measured the BMC and BMD of the whole body, femur, and tibia by dual-energy X-ray absorptiometry (DXA; Fig. 2a). As shown in Fig. 2a, the whole-body BMC ($n = 6$, $p = 0.000895$) and tibia BMC ($n = 6$, $p = 0.00149$) increased significantly in normal rats after supplementation with IR light. Although the femoral BMC failed to show a significant difference, it showed an increasing trend ($n = 6$, $p = 0.0575$). For ovariectomized rats, the BMC of the whole body ($n = 6$, $p = 2.55e{-}05$) increased significantly after IR supplemental light, with the tibia BMC ($n = 6$, $p = 0.0522$) also showing an increasing trend, while the femur BMC did not change significantly. This indicates that long-term, low-energy

IR supplementary light has a positive effect on whole body bone and tibial bone mass in both normal and ovariectomized rats.

The rat BMD measurements are provided in Fig. 2b. Inconsistent with the BMC results, the changes in femoral BMD were the most apparent; all significantly increased after IR supplementation (n = 6, Normal: p = 0.00229, Ovx: p = 0.00149). In contrast, the tibial BMD exhibited an increasing trend after IR supplementation, but was significant only in the normal rat group (n = 6, p = 0.000276). No significant changes in whole-body BMD were observed. These data indicate that long-term, low-energy IR supplementation has a positive effect on the local BMD, in both normal and ovariectomized rats, and can promote bone formation. Through micro-CT scanning to obtain the cross-sectional image of the distal femur, we can visualize the increase in trabecular bone density after infrared supplementation (Fig. 2c).

We also examined the changes in serum bone metabolism markers in the rats. The ovariectomized rats exhibited significant increases in $1,25(OH)_2D_3$ (n = 6, p = 0.0324) and BALP (n = 6, p = 2.26e−06) concentrations after exposure to the IR supplementary light (Fig. 2d). There was also an increasing trend in the normal rats, indicating that IR supplementation can increase the concentration of $1,25(OH)_2D_3$ and BALP in rats and has a positive effect on vitamin D synthesis and bone metabolism. Meanwhile, we observed increases in TRACP concentrations in both the normal + IR and ovariectomized +IR groups, suggesting that IR supplementation can increase the bone resorption rate in rats, regardless of the health of the bone.

Effects of IR supplementation on alpha diversity, beta diversity, and the microbial network

To evaluate the effects of IR irradiation on the richness and diversity of the gut microbiota, we compared the richness index (Chao1) and diversity index (Shannon_e) in each treatment group. The species abundance of the gut microbiota in both normal and ovariectomized rats significantly decreased after irradiation with the IR light (Fig. 3a). The Shannon_e index estimation indicates that IR irradiation and bone loss did not affect the gut microbiota diversity of the rats (Fig. 3b).

Based on the unweighted UniFrac distances of the OTU levels, we used Principal Coordinate Analysis (PCoA) to determine the effect of IR supplementation on the distribution of gut microbiota. As shown in Fig. 3c, we observed a separation of the microbiota between the white light-irradiated rats and IR-supplemented rats, whereas there was no apparent separation between the ovariectomized rats and normal rats. Similarity analysis between the different groups showed that IR supplementation had a highly significant effect on the composition of gut bacterial communities (ANOSIM, R = 0.8433, p = 0.001), and the effect is far greater than that of ovariectomy (ANOSIM, R = −0.011, p = 0.44).

We selected OTUs with relative abundance > 100 and used Spearman correlation coefficients to construct microbial interaction networks. Species analysis indicates that the four groups of networks are composed of bacteria from 4 phyla: Bacteroidetes, Firmicutes, Saccharibacteria, and Proteobacteria (Fig. 4). Table 1

presents the structural characteristics of the microbial networks in the different treatment groups. The microbial networks in both the normal and ovariectomized rats, after supplementation of IR, were significantly increased in degree and closeness centrality (Additional file 1: Figure S1). Meanwhile, supplementation with IR resulted in a larger average aggregation coefficient and a smaller average path length in both the normal and ovariectomized rats.

Taxon-based analysis of bacterial communities

To understand the types of bacteria in the rat intestine that could be affected by IR exposure, we analyzed the composition of the gut microbiota at the phylum and family levels (Fig. 3d, e). As shown in Fig. 3d, nine phyla of bacteria were detected in all four groups of rats, regardless of bone metabolism and IR exposure. Specifically, bacteria such as Firmicutes and Bacteroides were found as the dominant flora in the rat intestine. Saccharibacteria were found to be dramatically reduced in both normal and ovariectomized rats (Ovx: $p = 0.005$, Normal: $p = 0.002$) exposed to the IR light. The ratio of Firmicutes to Bacteriodetes showed a tendency to decrease (Additional file 1: Figure S2a). A total of 44 families have been annotated, of which 13 significantly changed. Fig. 3e shows the proportions of gut microbiota in each group at the family level. Interestingly, IR supplementation had a substantial impact on the gut microbiota, while ovariectomy did not (Additional file 1: Figure S3). We found that the relative abundance of *Clostridiaceae_1, Erysipelotrichaceae, Peptostreptococcaceae, Porphyromonadaceae,* and *Alcaligenaceae* all increased significantly after exposure to IR, while the relative abundance of *Desulforibrionaceae* decreased significantly (Additional file 1: Figure S2b). Meanwhile, there was a greater abundance of *Prevotellaceae* and *Lactobacillaceae* after exposure to IR, although these differences did not reach statistical significance.

We also assessed significant difference in genus after exposure to infrared. The IR exposure in both the normal and ovariectomized groups led to a decrease in *Candidatus_Saccharimonas* and an increase in *Clostridium_sensu_stricto_1, Turicibacter* and *Parabacteroides*Fig. 3f and g).

Functional prediction of metabolic pathway

The metabolism, genetic information processing, environmental information processing, cellular processes, organismal systems, and human disease pathways associated with the rat gut microbiota compositions were examined using the Tax4Fun software (Fig. 5, Additional file 2: Supplemental Table S1). The pathways annotated to metabolism accounted for the vast majority, of which Energy metabolism, Lipid metabolism, and metabolism of terpenoids and polyketides changed significantly in both ovariectomized and normal rats ($p < 0.05$). Next, we selected the top 60 pathways of relative abundance in metabolism, according to the KEGG pathway database (Additional file 1: Figure S4). IR supplementation significantly enriched the Butanoate metabolism, Propanoate metabolism, and Fatty acid biosynthesis pathways.

Correlation analysis between bone metabolism and the gut microbiome

In order to explore the relationship between gut microbiota and host physiology, we conducted Spearman correlation analysis, which revealed a significant correlation between the gut microbiota and bone metabolism. We selected the top 30 microorganism families, based on their relative abundance, and the families exhibiting significant differences between the different light treatment conditions all correlated well with bone metabolism (Fig. 6). *Erysipelotrichaceae, Clostridiaceae_1, Peptostreptococcaceae, Alcaligenaceae,* and *Porphyromonadaceae* positively correlated with bone indicators, while *Desulfovibrionaceae* negatively correlated with bone indicators. *Erysipelotrichaceae* and *Clostridiaceae_1* significantly correlated with all indexes except for whole-body BMD and Femur BMC ($p < 0.05$, $r > 0.4$) (Additional file 1: Figure S5). The remaining families exhibited relatively low abundances.

Discussion

Over the past decade, solid-state lighting sources based on white light-emitting diodes (LEDs) has gradually replaced incandescent and fluorescent lamps, becoming the main type of artificial light sources. Meanwhile, interest in the use of LED white lighting in human health has grown rapidly, as the concept of “healthy light” has developed [23,24]. Healthy lighting needs to take into account spectral regions outside the visible range, which have physiological and psychological impacts on humans, such as infrared radiation (IR), that is present in daylight but not white light-emitting LEDs [25]. Previous studies have demonstrated the potential value of infrared radiation from laser light in the prevention of bone loss in animal models [26,27] or in elderly osteoporosis patients [28]. These studies suggest that IR supplementation to white LEDs may be beneficial in creating an artificial lighting environment conducive to the maintenance of bone health. Motivated by this, in the present study, we investigated the effect of IR supplementation to white LEDs on the bone health of rats. We found some degree of increase in the BMC and BMD in both normal and ovariectomized rats after IR supplementation (Fig. 2). These results are in agreement with a previous report that IR laser therapy improves bone synthesis in osteoporotic as well as in normal rats [29]. Interestingly, serum bone metabolism biomarkers, including 1,25 (OH) 2D3, BALP, and TRACP, were significantly increased, especially in ovariectomized rats (Fig. 3), indicating that IR promotes not only bone formation but also bone resorption.

The mechanisms involved in the benefits of IR exposure to bone health have been widely investigated. It is generally accepted that IR can effectively increase the activity of cytochrome oxidase and mitochondrial ATP production, and accelerate bone formation by increasing local vascularization and the organization of collagen fibers [28,30]. However, these processes are not just manifested in bone tissue to explain the mechanism. IR can produce significant systemic effects, whereby the beneficial effects on bone tissue may occur via other tissues.

In recent years there has been accumulating evidence that the gut microbiome is a key regulator of bone health [31–33]. To better understand the role of gut flora in the improvement of bone through IR exposure, we analyzed the effect of IR irradiation on gut microbiota and analyzed the correlation between microbiota changes and bone morphology and metabolism.

Diversity analysis and network analysis are valuable tools in quantifying the bacterial composition and interaction of specific bacterial communities. Our investigation of alpha diversity revealed a decreasing trend of diversity estimators in both the normal and ovariectomized groups after IR supplementation (Fig. 4a-b). Similarly, PCoA analysis of beta diversity was able to discriminate the IR supplementary groups from the non-IR supplementary groups (Fig. 4c). These results suggest that a less diverse gut microbiome after IR exposure may be related to the increase in bone mass. Previous studies have demonstrated a negative association between gut microbiota biodiversity and BMD in humans [34–36]. We also found that IR-induced co-occurrence networks of gut microbiota in both normal and ovariectomized rats were characterized by properties that indicate higher compactness, stronger aggregation, and larger transmission efficiency, such as high degree and closeness centrality, large average aggregation coefficients, and small average paths (Additional file 1: Figure S1, Table 1). Therefore, we speculate that chronic IR exposure can induce the emergence of a distinct, stable community underpinned by more complex interaction networks and faster communication between nodes [37].

Table 1
Network structure characteristics

	No. of nodes	No. of edges	Average degree	Diameter	Density	Modularity class	Average clustering coefficient	Average path length
Normal	46	76	3.304	12	0.073	2.539	0.413	4.538
Normal+IR	51	143	5.508	8	0.112	1.624	0.558	3.411
Ovx	52	83	3.192	11	0.063	1.998	0.48	4.795
Ovx+IR	54	164	6.074	8	0.115	1.944	0.557	2.988

With respect to the phylum level of the gut microbial community in rats, we found that the quantity Saccharibacteria (formerly TM7) [38] was significantly reduced after IR supplementation (Fig. 3d). Volcano plot results further show that both the normal and ovariectomized rats exhibited a significant decrease in the content of a bacterium (i.e., *Candidatus_Saccharimonas,* the major genus of Saccharibacteria) after IR supplementation (Fig. 3f-g). In addition, the ratio of Firmicutes to Bacteroidetes showed a decreasing trend. Previous studies have shown that Saccharibacteria is related to the body's immune response [39] and the occurrence of some inflammatory mucosal diseases, such as vaginosis and inflammatory bowel disease [40–42], while the ratio of Firmicutes to Bacteroidetes gut microbiota is indicative of dysregulation of various biological processes, such as maintenance of bone volume [43]. As this ratio increases, intestinal permeability may be altered, leading to greater susceptibility to disease.

At the family level, supplemental IR increases the abundance of specific classification operating units, including *Clostridiaceae* 1, *Erysipelotrichaceae, Peptostreptococcaceae, Porphyromonadaceae* and *Prevotellaceae* (Additional file 1: Figure S2). *Clostridiaceae* and *Peptostreptococcaceae* are involved in maintaining the intestinal barrier [44]. Moreover, some bacteria in the *Clostridiaceae* family have been shown to be involved in the production of butyric acid and the degradation of mucin, thus contributing to improved

gut health [45]. Butobaric acid producers, including *Allobaculum* and *Turicibacter*,account for the vast majority in the family *Erysipelotrichaceae* [46]. *Prevotellaceae* is also considered to be related to the synthesis of short-chain fatty acids (SCFAs) [47]. Butyrate is a short-chain fatty acid (SCFA) that has been used to treat metabolic disorders, such as obesity, insulin resistance, and postmenopausal osteoporosis [48,49]. It has been found that modulating the gut microbiome to increase butyric acid production can enhance the integrity and function of the intestinal barrier, thereby improving periodontal bone loss [50]. Other studies have shown that the metabolite, butyrate, can stimulate bone formation through regulatory T cell-mediated WNT10B expression [51]. Additionally, *Porphyromonadaceae* have been negatively correlated with TNF-α expression [52]. TNF-α plays an important role in the regulation of bone homeostasis, mainly by stimulating complex signaling pathways to induce the transcription and expression of bone homeostasis regulators [53]. Increased levels of TNF-α can inhibit the osteogenic differentiation of bone marrow mesenchymal stem cells, resulting in osteoporosis [54]. *Parabacteroides* is an important genus in the *Porphyromonadaceae* family, which has also been shown to negatively correlate with some inflammatory diseases and may play a positive regulatory role in the metabolism of glycolipids [55].

The abundance of *Desulfovibrionaceae* decreased significantly after exposure to IR. These bacteria can induce the production of H_2S from sulfate compounds during anaerobic respiration [56]. H_2S interferes with the energy metabolism of intestinal epithelial cells, eventually causing cell death and an accompanying intestinal inflammation [57]. We present our working model in Fig. 7, which is a schematic of the effect of light exposure on the gut-bone axis. We propose that changes in the gut microbiota mediated by IR affects the expression of intestinal immune factors and microbial metabolites, such as short-chain fatty acids and H_2S, which may be beneficial to bone metabolism and have relevance in the treatment of osteoporosis. Finally, we found *Erysipelotrichaceae, Clostridiaceae*_1, and *Porphyromonadaceae* to be significantly positively correlated with the increase in BMC and BMD in rats (Fig. 6), suggesting that the IR-induced increase of these bacteria also aid in bone formation.

Changes in bacterial community function can help us further understand the effects of gut microbiota on bone metabolism in rats treated with IR supplementation. In both normal and ovariectomized rats, butanoate metabolism, propanoate metabolism, and fatty acid biosynthesis pathways were all enriched after IR supplementation (Additional file 1: Figure S4). Butyric acid and propionic acid are SCFAs and secondary metabolites produced by gut microbiota during carbohydrate fermentation. Previous studies have shown that supplementation with SCFAs, especially propionic acid and butyric acid, can balance bone homeostasis, increase bone mass, and prevent bone loss, which lends further support to our conclusions [49].

Conclusion

In summary, our report is the first to identify compositional and functional alterations in the gut microbiota in both normal and ovariectomized rats by IR supplementation to white LED exposure. The induction of key gut microbes by IR supplementation is associated with improved bone metabolism through a reduction in inflammation and an increase in butyrate production. In addition to suggesting a previously unappreciated

mediatory role of gut microbiota between IR and bone metabolism, our findings may be immediately relevant to the design of healthy lighting environments for the prevention of osteoporosis. Of note, our results were obtained in an experimental rat model, and it will be necessary to perform intensive investigations in human subjects. The gut microbiota-mediated molecular mechanisms behind the beneficial bone health effects of IR must be further elucidated, and the identified bacterial markers in the gut are deserving of future validation.

List Of Abbreviations

UVR: Ultraviolet irradiation

IR: infrared radiation

LED: white light-emitting diodes

Ovx: ovariectomized

BMC: bone mass content

BMD: bone mineral density

1,25-(OH)2-D3: 1,25-dihydroxyvitamin D3

BALP bone-specific alkaline phosphatase

TRACP: tartrate-resistant acid phosphatase

OTU: operational taxonomic unit

PcoA: principal coordinate analysis

SCFAs: short-chain fatty acids

Declarations

Ethics approval and consent to participate

All animal experiments were performed with approval by the Science and Ethics Committee of School of Beihang University (Approval ID: BM20180003).

Consent for publication

Not applicable.

Availability of data and material

The datasets supporting the conclusions of this article are available in the NCBI SRA repository, [Accession numbers SRP262880; http://ncbi.nlm.nih.gov/sra/].

Competing interests

The authors declare that they have no competing interests.

Funding

This work was financially supported by a grant from the National Natural Science Foundation of China (31870852) and the Fundamental Research Funds for the Central Universities.

Authors' contributions

YL performed sample collection, data analysis, and wrote the manuscript; JY performed sample collection and preliminary data processing and analysis; YF and HL designed the experiments and reviewed the manuscript. All authors read and approve of the final manuscript.

Acknowledgements

This work was financially supported by the grants from the National Natural Science Foundation of China (81871520, 31870852).

References

1. Terzi R, Yılmaz Z. Bone mineral density and changes in bone metabolism in patients with obstructive sleep apnea syndrome. Journal of bone and mineral metabolism, 2016, 34(4): 475-481.
2. Luria T, Matsliah Y, Adir Y, et al. Effects of a Prolonged Submersion on Bone Strength and Metabolism in Young Healthy Submariners. Calcified Tissue International, 2010, 86(1):8-13.
3. Mccoll S, A. Veitch J. Full-spectrum fluorescent lighting: a review of its effects on physiology and health. Psychological Medicine, 2001, 31(6):949-964.
4. MF H. Biological Effects of Sunlight, Ultraviolet Radiation, Visible Light, Infrared Radiation and Vitamin D for Health. Anticancer research, 2016,36(3):1345-1356.
5. Morita D, Higuchi Y, Makida K, Seki T, Ikuta K, Ishiguro N, Nishida Y. Effects of ultraviolet irradiation with a LED device on bone metabolism associated with vitamin D deficiency in senescence-accelerated mouse P6. Heliyon. 2020 Feb 28;6(2): e03499.

6. Rong, Guo, Yao, et al. The effects of ultraviolet supplementation to the artificial lighting on rats' bone metabolism, bone mineral density, and skin. Journal of Photochemistry & Photobiology B Biology, 2018.
7. Bosman E S, Albert A Y, Lui H, et al. Skin exposure to Narrow Band Ultraviolet (UV) B light modulates the human intestinal microbiome. Frontiers in microbiology, 2019, 10: 2410.
8. Hamblin M R. Mechanisms and applications of the anti-inflammatory effects of photobiomodulation. AIMS biophysics, 2017,4(3):337-361.
9. Patra V, Laoubi L, Nicolas J, et al. A Perspective on the Interplay of Ultraviolet-Radiation, Skin Microbiome and Skin Resident Memory TCRαβ+ Cells. Frontiers in Medicine, 2018, 5:166-.
10. Clark A, Mach N. Role of Vitamin D in the Hygiene Hypothesis: The Interplay between Vitamin D, Vitamin D Receptors, Gut Microbiota, and Immune Response. Frontiers in immunology, 2016,7:627.
11. Pinheriro A, Limeira Junior Fde A, Gerbi ME, Ramalho LM, Marzola C, Ponzi E. Effect of low-level laser therapy on the repair of bone defected grafted with inorganic bovine bone. Braz Dent J, 2003,14:177–181.
12. Ueda Y, Shimizu N. Effects of pulse frequency of low-level laser therapy (LLLT) on bone nodule formation in rat calvarial cells. Journal of clinical laser medicine & surgery, 2003, 21(5): 271-277.
13. Cyborg Nicholson JK, Holmes E, Wilson ID. Gut microorganisms, mammalian metabolism and personalized health care. Nature Reviews Microbiology, 2005, 3(5):431-438.
14. Zhuang H, Li Y, Huang H X, et al. Correlation between body mass and bone mineral density in ovariectomized rats. Journal of Clinical Rehabilitative Tissue Engineering Research, 2008, 12(24):4655-4658.
15. Rognes T, Flouri T, Nichols B, et al. VSEARCH: a versatile open source tool for metagenomics. PeerJ, 2016, 4: e2584.
16. Quast C, Pruesse E, Yilmaz P, et al. The SILVA ribosomal RNA gene database project: improved data processing and web-based tools. Nucleic acids research, 2013,41(Database issue):D590-D596.
17. E. J. Newman. Modularity and community structure in networks. Proceedings of the National Academy of ences of the United States of America, 2006, 103(23):8577-8582.
18. Mathieu Bastian, Sebastien Heymann, Mathieu Jacomy. Gephi: An Open Source Software for Exploring and Manipulating Networks. Proceedings of the Third International Conference on Weblogs and Social Media, ICWSM 2009, San Jose, California, USA, May 17-20, 2009. 2009.
19. Aßhauer K P, Wemheuer B, Daniel R, et al. Tax4Fun: predicting functional profiles from metagenomic 16S rRNA data. Bioinformatics, 2015,31(17):2882-2884.
20. Sharpton, Thomas, J. An introduction to the analysis of shotgun metagenomic data. Frontiers in Plant Science, 2014.
21. Ihaka R, Gentleman R. R: A Language for Data Analysis and Graphics. Journal of Computational and Graphical Statistics, 1996,5(3):299-314.
22. CLARKE K R. Non-parametric multivariate analyses of changes in community structure. Australian Journal of Ecology, 1993,18(1):117-143.

23. Hye Oh J, Ji Yang S, Rag Do Y. Healthy, natural, efficient and tunable lighting: four-package white LEDs for optimizing the circadian effect, color quality and vision performance. Light Science & Applications, 2014, 3(2): e141.
24. Tingzhu W, Yue L, Honghui Z, et al. Multi-function indoor light sources based on light-emitting diodes–a solution for healthy lighting. Optics Express, 2016, 24(21):24401-.
25. Zielinska-Dabkowska, Karolina, M. Make lighting healthier. Nature, 2018.
26. Renno A C M, Moura F M D, Santos, Nádia Slemer Andrade Dos, et al. Effects of 830-nm Laser Light on Preventing Bone Loss after Ovariectomy. Photomedicine & Laser Surgery, 2006, 24(5):642-645.
27. Mohsenifar Z, Fridoni M, Ghatrehsamani M, et al. Evaluation of the effects of pulsed wave LLLT on tibial diaphysis in two rat models of experimental osteoporosis, as examined by stereological and real-time PCR gene expression analyses. Lasers in Medical Science, 2016,31(4):721-732.
28. Abdelaal A, Taha M, Amin D, et al. Effect of pulsed electromagnetic therapy versus low-level laser therapy on bone mineral density in the elderly with primary osteoporosis: a randomized, controlled trial. Bulletin of Faculty of Physical Therapy, 2017,22(1):34-39.
29. Saad A, Yamany M E, Abbas O, et al. Possible role of low level laser therapy on bone turnover in ovariectomized rats. Endocrine regulations, 2010, 44(4):155-163.
30. Ann Liebert, Brian Bicknell, Daniel M. Johnstone, et al. "Photobiomics": Can Light, Including Photobiomodulation, Alter the Microbiome? Photobiomodulation, photomedicine, and laser surgery, 2019, **37**(11): 681-693.
31. Yan J, Herzog J W, Tsang K, et al. Gut microbiota induce IGF-1 and promote bone formation and growth. Proceedings of the National Academy of Sciences, 2016:201607235.
32. Hsu E, Pacifici R. From Osteoimmunology to Osteomicrobiology: How the Microbiota and the Immune System Regulate Bone. Calcified Tissue International, 2018, 102(5):512-521.
33. Yan J, Takakura A, Zandi-Nejad K, et al. Mechanisms of gut microbiota-mediated bone remodeling. Gut Microbes, 2017:1-9.
34. Jihan, Wang, Yangyang, et al. Diversity analysis of gut microbiota in osteoporosis and osteopenia patients. Peerj, 2017, **5**: e3450.
35. Das M, Cronin O, Keohane D M, et al. Gut microbiota alterations associated with reduced bone mineral density in older adults. Rheumatology, 2019,58(12):2295-2304.
36. Lin X, Xiao H, Liu H, et al. Gut microbiota impacts bone via B.vulgatus-valeric acid-related pathways. 2020.
37. Fronczak, Agata, Fronczak, Piotr, Ho?yst, Janusz A. Average path length in random networks. Physical Review E, 2004, 70(5):056110.
38. Bor B, Bedree J K, Shi W, et al. Saccharibacteria (TM7) in the Human Oral Microbiome. Journal of Dental Research, 2019,98(5):500-509.
39. Kuehbacher T, Rehman A, Lepage P, et al. Intestinal TM7 bacterial phylogenies in active inflammatory bowel disease. Journal of Medical Microbiology, 2008, 57(12):1569-1576.

40. Brinig M M, Lepp P W, Ouverney C C, et al. Prevalence of Bacteria of Division TM7 in Human Subgingival Plaque and Their Association with Disease. Applied and Environmental Microbiology, 2003,69(3):1687.
41. Kuehbacher T, Rehman A, Lepage P, et al. Intestinal TM7 bacterial phylogenies in active inflammatory bowel disease. Journal of Medical Microbiology, 2008,57(12):1569-1576.
42. Fredricks D N, Fiedler T L, Marrazzo J M. Molecular Identification of Bacteria Associated with Bacterial Vaginosis. New England Journal of Medicine, 2005,353(18):1899-1911.
43. David Yatsonsky , Karen Pan, Vithal B Shendge, et al. Linkage of microbiota and osteoporosis:A mini literature review. World Journal of Orthopedics, 2019, 10(03):4-8.
44. Wlodarska, Marta, Willing, Benjamin P, Bravo, David M, et al. Phytonutrient diet supplementation promotes beneficial Clostridia species and intestinal mucus secretion resulting in protection against enteric infection. Scientific Reports, 2015, 5:9253.
45. Levine U Y, Looft T, Allen H K, et al. Butyrate-producing bacteria, including mucin degraders, from the swine intestinal tract. Applied and environmental microbiology, 2013,79(12):3879-3881.
46. Elena H, Wayne Y, Verena R G, et al. In Vivo Assessment of Resistant Starch Degradation by the Caecal Microbiota of Mice Using RNA-Based Stable Isotope Probing—A Proof-of-Principle Study. Nutrients, 2018, 10(2):179-.
47. Shen F, Zheng RD, Sun XQ, et al. Gut microbiota dysbiosis in patients with non-alcoholic fatty liver disease. Hepatobiliary Pancreat Dis Int 2017;16(4):375-381.
48. McNabney M S, Henagan M T. Short Chain Fatty Acids in the Colon and Peripheral Tissues: A Focus on Butyrate, Colon Cancer, Obesity and Insulin Resistance: Nutrients. 2017: 9.
49. Lucas S, Omata Y, Hofmann J, et al. Short-chain fatty acids regulate systemic bone mass and protect from pathological bone loss. Nature Communications, 2018,9(1):55.
50. Jia X, Jia L, Mo L, et al. Berberine Ameliorates Periodontal Bone Loss by Regulating Gut Microbiota. Journal of Dental Research, 2018,98(1):107-116.
51. Tyagi A M, Yu M, Darby T M, et al. The Microbial Metabolite Butyrate Stimulates Bone Formation via T Regulatory Cell-Mediated Regulation of WNT10B Expression. Immunity, 2018,49(6):1116-1131.
52. Zhang, X., Wang, H., Yin, P. *et al.* Flaxseed oil ameliorates alcoholic liver disease via anti-inflammation and modulating gut microbiota in mice. Lipids Health Dis, 2017, 16,
53. Paula Rozenfeld, Juan Mucci, Pablo De Francesco, et al. Study of the Mechanisms of Osteoclastogenesis Induction in an In Vitro Model of Gaucher Disease. Molecular Genetics & Metabolism, 2012, 105(2).
54. Deng L, Hu G, Jin L, Wang C, Niu H. Involvement of microRNA-23b in TNF-α-reduced BMSC osteogenic differentiation via targeting runx2. *J Bone Miner Metab*. 2018;36(6):648-660.
55. M, Kverka, Z, et al. Oral administration of Parabacteroides distasonis antigens attenuates experimental murine colitis through modulation of immunity and microbiota composition. Clinical & Experimental Immunology, 2010.

56. Wagner M, Roger AJ, Flax JL, Brusseau GA, Stahl DA. Phylogeny of dissimilatory sulfite reductases supports an early origin of sulfate respiration. J Bacteriol 1998; 180: 2975-2982.
57. Babidge W, Millard S, Roediger W. Sulfides impair short chain fatty acid beta-oxidation at acyl-CoA dehydrogenase level in colonocytes: implications for ulcerative colitis. Mol Cell Biochem 1998; 181: 117-124.

Figures

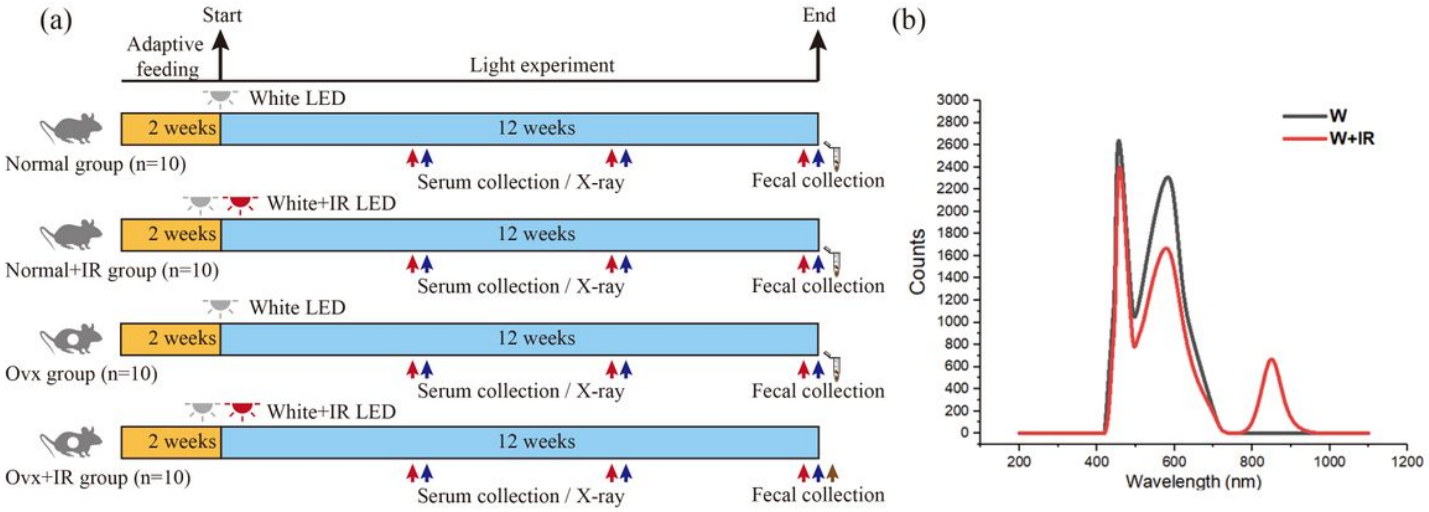

Figure 1

(a) Experimental design for the three-month LED exposure experiment. The red arrows indicate the monthly serum collection, while the blue arrows represent the monthly bone mass and density measurements. At the end of the experiment, fecal samples were acquired for high-throughput sequencing. (b) LED white light spectrum and LED white light plus IR spectrum.

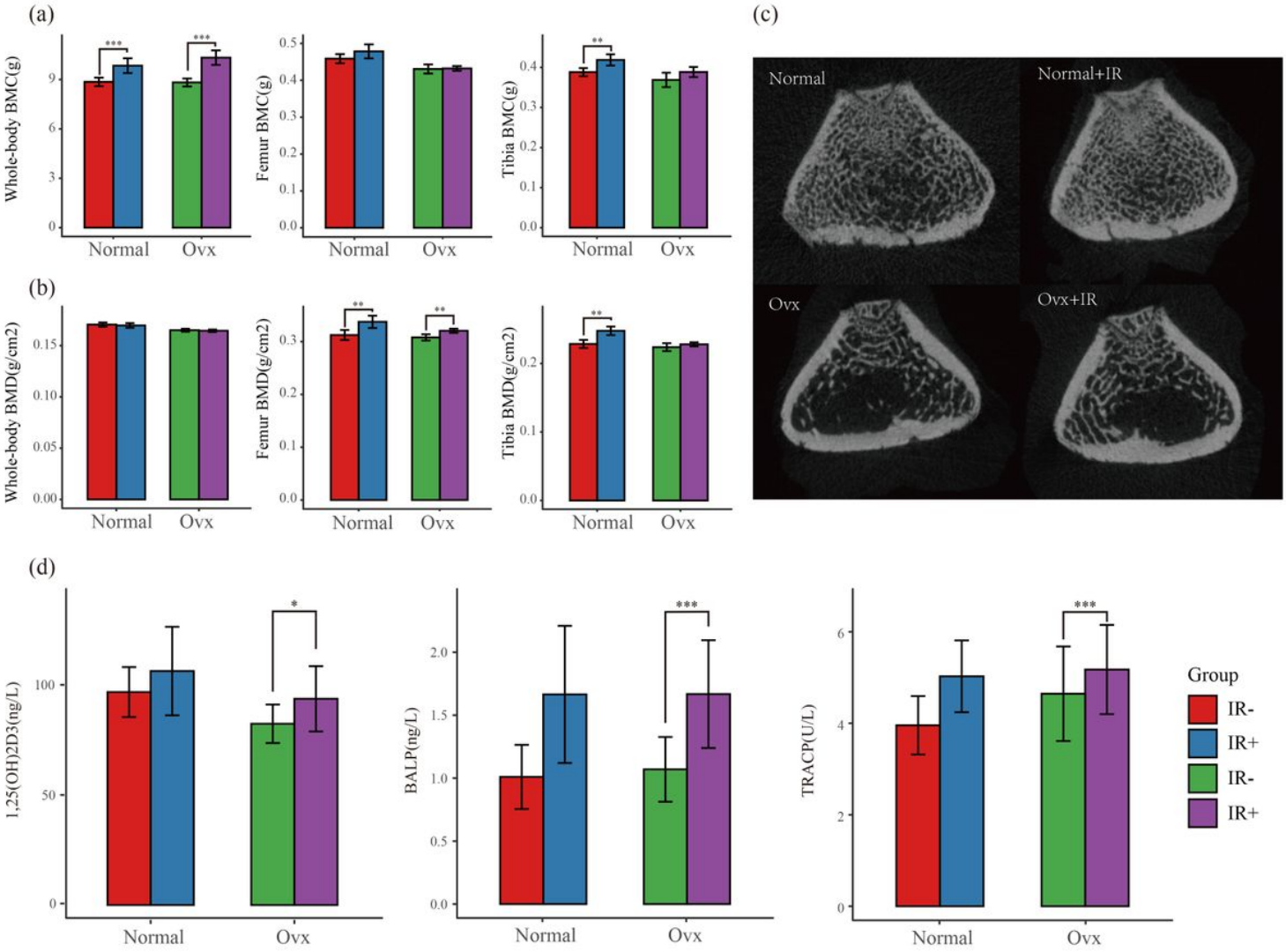

Figure 2

Measurements of (a) BMC and (b) BMD in the whole body, femur, and tibia of rats. (c) Representative images of the trabecular bone density from the distal metaphyseal region of the femur. (d) The concentration changes in serum bone metabolism markers: 1,25(OH)2D3, BALP, TRACP. *p<0.05, **p<0.01, ***p<0.001.

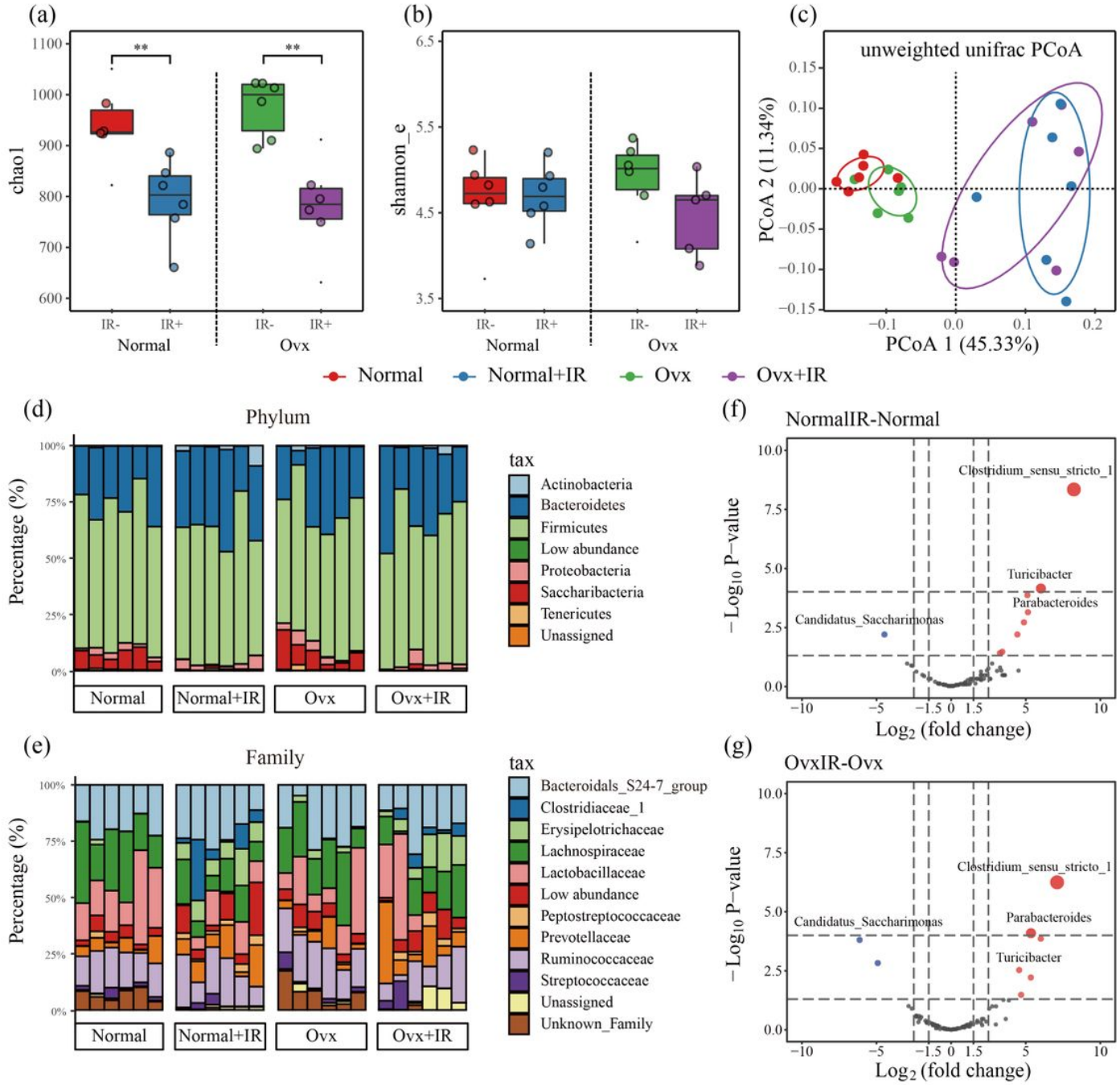

Figure 3

Comparison of bacterial OTUs (operational taxonomic units) between the normal and ovariectomized (Ovx) rats: (a) Alpha diversity based on Chao1 index; (b) Alpha diversity using the Shannon_e index; (c) Principal Coordinate Analysis (PCoA) of weighted UniFrac distances of gut microbiota. Analysis of the microbial taxa composition after the indicated treatments, based on 16S rRNA gene sequencing at the (d) phylum and (e) family levels. Genera showing significant differences in (f) normal and (g) ovariectomized rats with and without IR treatment.

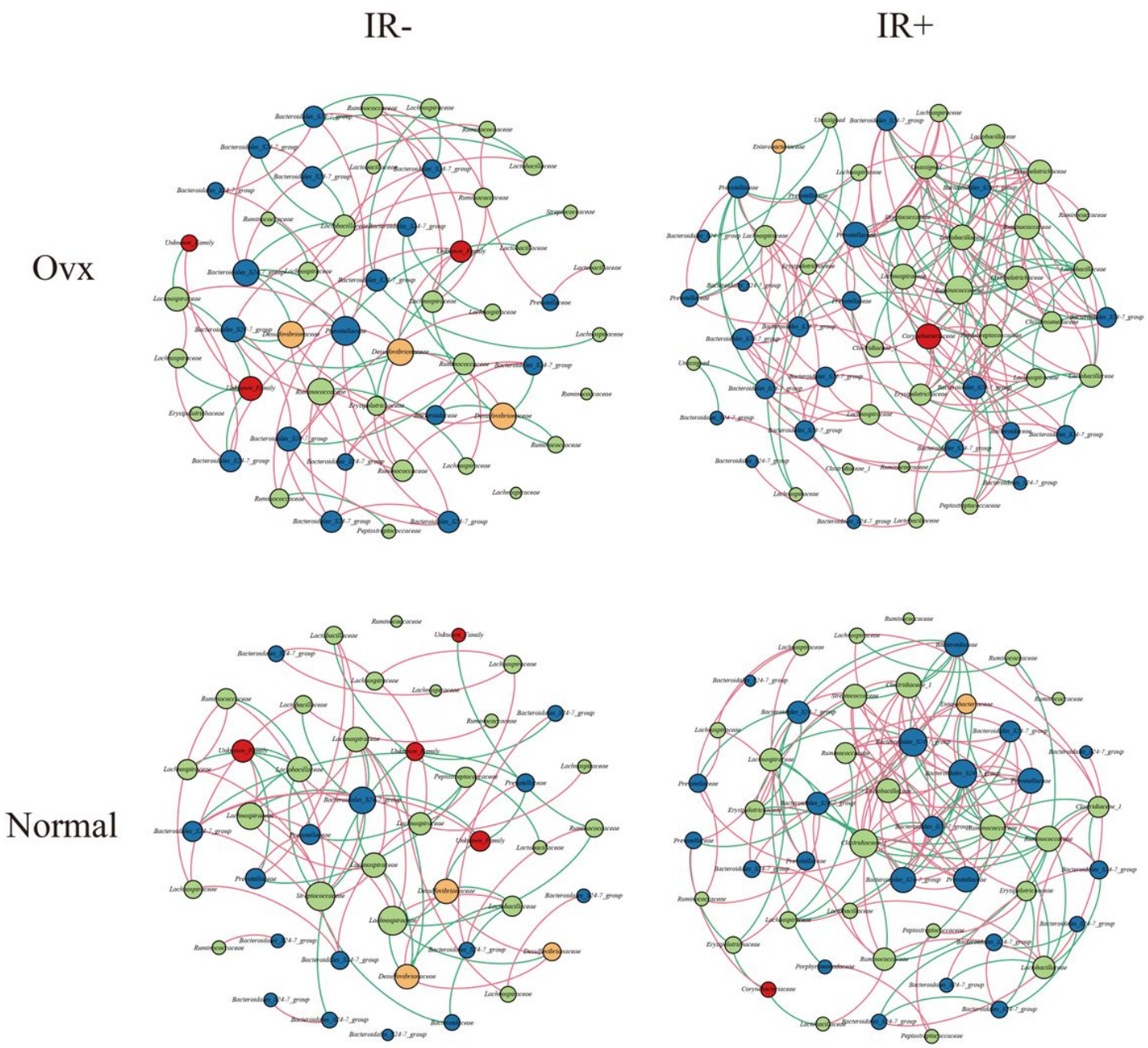

Figure 4

Bacterial network of the indicated treatment groups. Nodes represent OTUs; node size represents connectivity; colors represent different phylum levels. Edges (connections): red represents positive correlation, green represents negative correlation (Spearman). (| r | > 0.7, p<0.05).

Figure 5

Predictive functional profiling of microbial communities by Tax4Fun analysis. The ordinate shows the primary metabolic pathways and their respective secondary pathways. * p <0.01, **p<0.05.

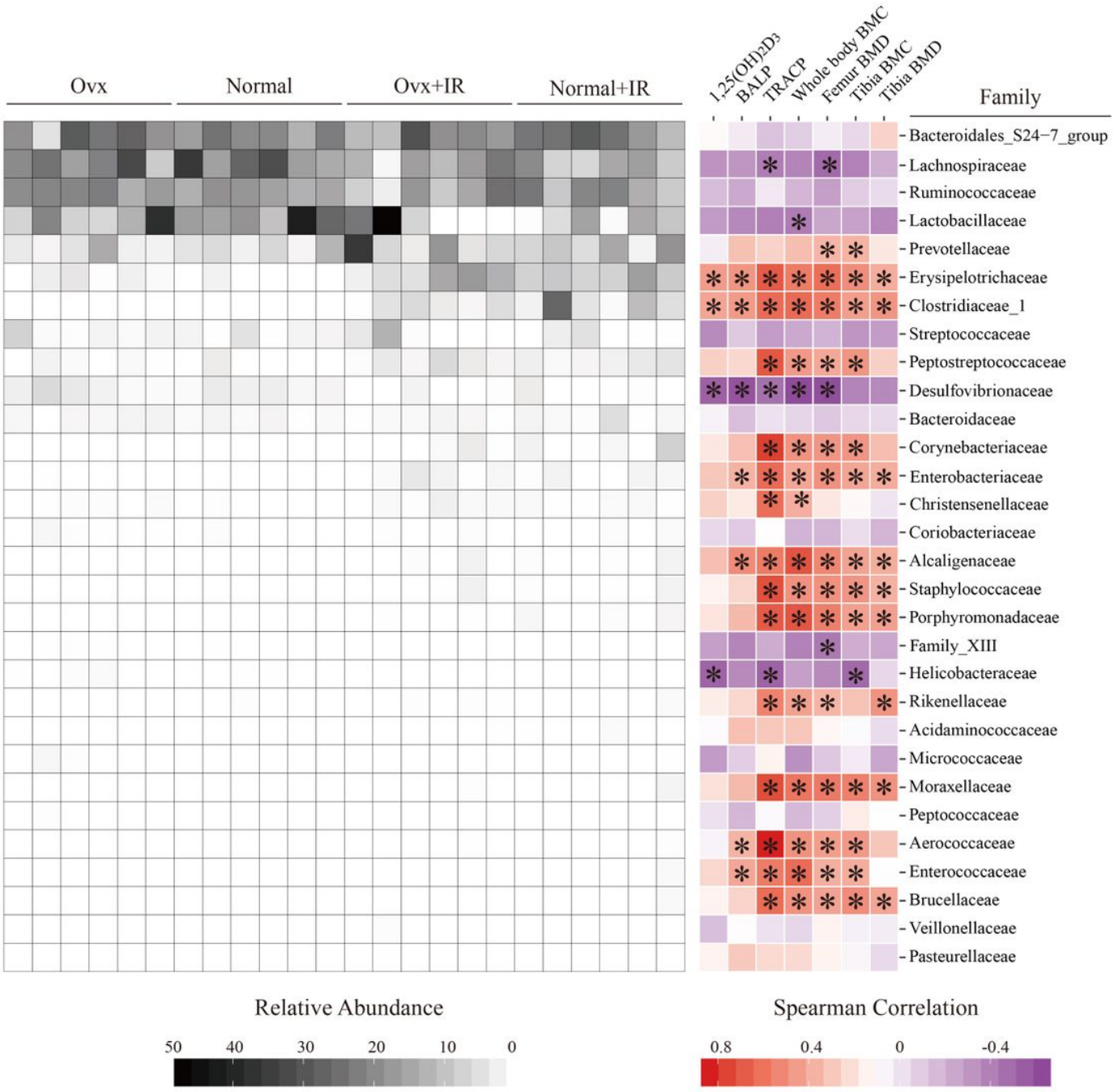

Figure 6

Spearman correlation analysis. The correlation of the gut microbiota distribution with the four experimental groups was examined at the family level. The heat map on the left shows the relative abundance of each family, while the right hand panel shows the Spearman correlation between family and bone metabolism index. Red indicates a positive correlation, whereas purple designates a negative correlation. The shading intensity of the squares indicates the Spearman rank correlation coefficient between matrices. *p < 0.05.

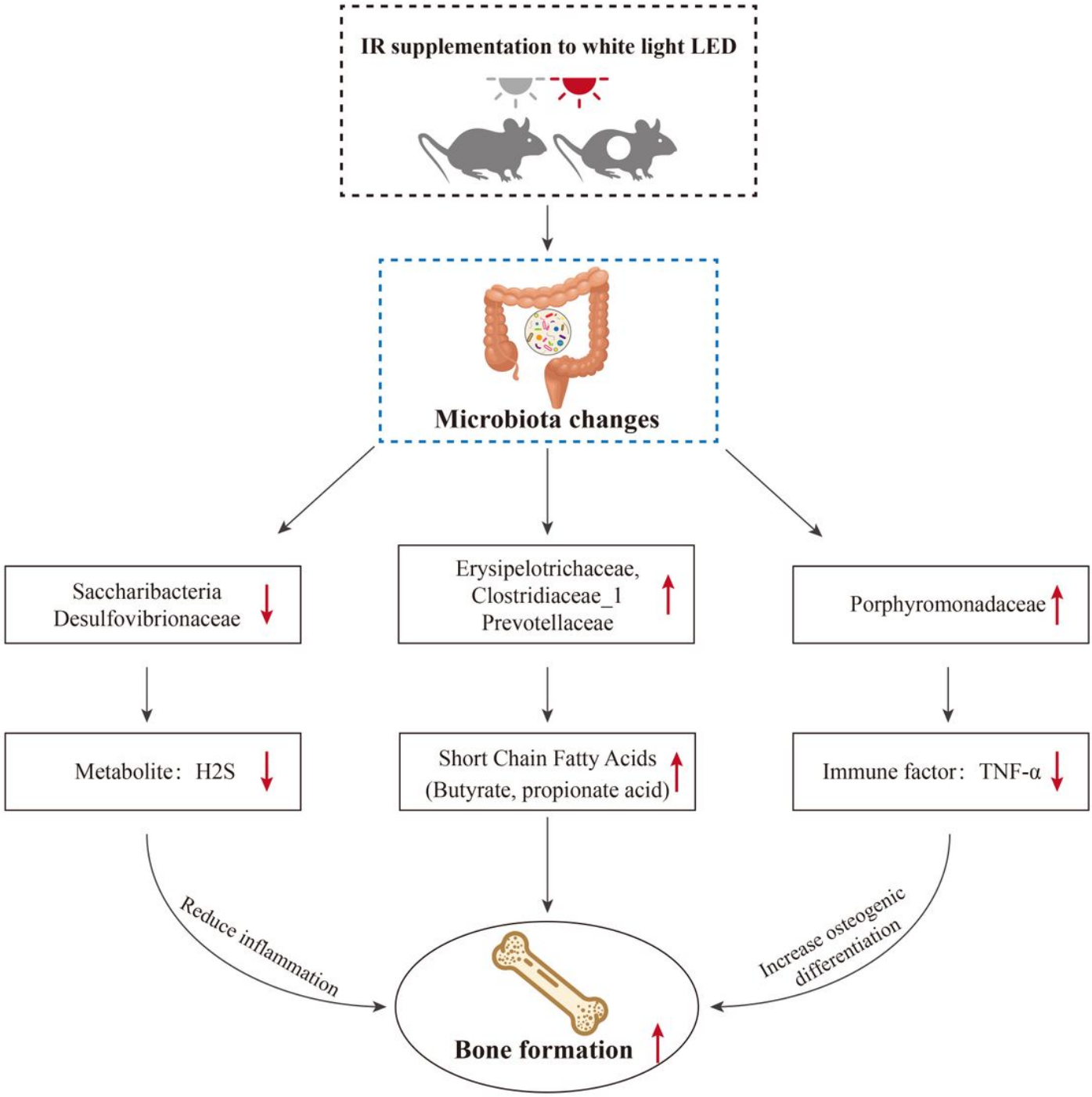

Figure 7

Proposed mechanisms of IR effects through the skin-gut-bone axis.

Supplementary Files

This is a list of supplementary files associated with this preprint. Click to download.

- additionalfile2.xlsx
- additionalfile2.xlsx
- additionalfile2.xlsx
- additionalfile1.docx
- additionalfile1.docx
- additionalfile1.docx